Atmospheric Chemistry of HFC-134a: Kinetic and Mechanistic Study of the $CF_3CFHO_2 + HO_2$ Reaction

M. Matti Maricq,* Joseph J. Szente, Michael D. Hurley, and Timothy J. Wallington*

Research Laboratory, Ford Motor Company, P.O. Box 2053, Drop 3083, Dearborn, Michigan 48121

Received: April 14, 1994; In Final Form: June 30, 1994®

Rate constant measurements for the title reaction and for $F + CF_3CFH_2$ are reported over the 210–363 K temperature range. Reacting mixtures of CF_3CFHO_2 and HO_2 radicals are created by the flash photolysis of F_2 in the presence of HFC-134a (CF_3CFH_2), H_2, and O_2 and are probed by time-resolved UV absorption spectroscopy. The deconvolution of spectra taken at various delay times provides concentration versus time profiles for the respective radical species. A comparison of the initial CF_3CFHO_2 and HO_2 concentrations yields a relative rate determination of $k_1 = (9.8^{+9}_{-5}) \times 10^{-11}e^{(-1130\pm190)/T}$ cm^3 s^{-1} for the $F + CF_3CFH_2$ rate constant. A simultaneous fit of the radical decay curves to a mechanism containing the known HO_2 self-reaction kinetics, the previously determined CF_3CFHO_2 self-reaction mechanism, and a cross reaction between these species yields a rate constant of $k_7 = (1.8^{+2.4}_{-1.0}) \times 10^{-13}e^{(910\pm220)/T}$ cm^3 s^{-1} for the $HO_2 + CF_3CFHO_2$ reaction. A product study at 296 K by Fourier transform infrared spectroscopy reveals that less than 5% of the product appears as $CF_3C(O)F$. By inference, >95% of the reaction gives the hydroperoxide $CF_3CFHOOH$. Implications of these results are discussed with respect to the atmospheric degradation of HFC-134a (CF_3CFH_2).

I. Introduction

Chlorofluorocarbon compounds (CFCs) pose a threat to the ozone layer because their chemical inertness in the atmosphere provides a mechanism for transporting chlorine from the earth's surface to the stratosphere, where photodissociation of the CFCs releases chlorine atoms to participate in ozone depletion. Strategies for CFC replacements have sought to overcome this problem by introducing compounds that are reactive in the troposphere yet retain the physical properties that made the CFCs useful in their original applications. For this strategy to be environmentally acceptable, the atmospheric consequences of the reactivity of the replacements must be examined, and indeed, this question has been at the center of considerable research activity over the past few years.[1]

HFC-134a (CF_3CFH_2) is the principal CFC replacement for air conditioning applications, and it is already being introduced in new model automobiles. Because it contains hydrogen atoms, HFC-134a reacts with OH radicals in the troposphere to produce an alkyl radical which rapidly adds molecular oxygen to form CF_3CFHO_2. At this point a variety of reaction paths are possible:

$$CF_3CFHO_2 + NO \rightarrow CF_3CFHO + NO_2$$

$$CF_3CFHO_2 + NO_2 \rightleftarrows CF_3CFHO_2NO_2$$

$$CF_3CFHO_2 + HO_2 \rightarrow CF_3CFHOOH + O_2$$

$$\rightarrow CF_3C(O)F + H_2O + O_2$$

$$CF_3CFHO_2 + RO_2 \rightarrow CF_3CFHO + RO + O_2$$

$$\rightarrow CF_3C(O)F + ROH + O_2$$

$$\rightarrow CF_3CFHOH + R'C(O)X + O_2$$

While the most important of these is presumed to be the reaction with NO, little kinetic data are actually available for these reactions. The rate constant of $(1.28 \pm 0.36) \times 10^{-11}$ cm^3 s^{-1} at 295 K, reported by Wallington and Nielsen,[2] indicates that the CF_3CFHO_2 reaction with NO is moderately fast, as expected from comparison to analogous reactions for other peroxy radicals.[3,4]

A more complete understanding of the fate of the peroxy radical from HFC-134a awaits data on the remainder of the above peroxy reaction channels. Because the atmospheric lifetimes of alkylperoxy nitrates are typically short[1,3,4] and since atmospheric concentrations of peroxy radicals are relatively small, the next most important channel is arguably the reaction with HO_2. NO concentrations outweigh those of HO_2 in urban areas, but the latter become relatively more important in remote areas. Hayman[5] has reported a preliminary room temperature rate constant for this reaction which suggests that the HO_2 reaction with CF_3CFHO_2 is slower than its reaction with most other peroxy radicals. However, since most $RO_2 + HO_2$ reactions exhibit a negative temperature dependence, reliance on a room temperature rate constant could underestimate the importance of the HO_2 reaction channel. In this paper we report $CF_3CFHO_2 + HO_2$ reaction rate constants measured over the temperature range 210–363 K by time-resolved UV spectroscopy. The description of the technique and the method for deconvoluting the spectra to obtain concentration versus time profiles are reviewed in section II. A brief overview of the FTIR smog chamber is also presented. The results of the kinetic measurements and of the product study for the title reaction are given in section III along with the kinetic data for $F + CF_3CFH_2$. The atmospheric implications are discussed in section IV.

II. Experimental Section

A. Real Time Kinetics. The flash photolysis–time-resolved UV spectrometer used in these experiments has been previously described.[6,7] An approximately 400 mJ pulse of 351 nm radiation is directed coaxially through a jacketed and insulated fused silica cell which measures 3.2 cm in diameter by 51 cm in length. This pulse dissociates approximately 0.25% of the F_2 in a $F_2/CF_3CFH_2/H_2/O_2/N_2$ gas mixture and initiates the following sequence of reactions:

$$F + CF_3CFH_2 \rightarrow CF_3CFH + HF \quad (1)$$

* To whom correspondence should be addressed.
® Abstract published in *Advance ACS Abstracts*, August 1, 1994.

0022-3654/94/2098-8962$04.50/0

TABLE 1: $CF_3CFHO_2 + HO_2$ Reaction Mechanism

reaction[a]	rate constant
1. $F + CF_3CFH_2 \rightarrow CF_3CFH + HF$	$k = 9.8 \times 10^{-11} e^{-1130/T}$ cm^3 s^{-1} [b]
2. $F + H_2 \rightarrow H + HF$	$k = 1.7 \times 10^{-10} e^{-550T}$ cm^3 s^{-1} 13
3. $CF_3CFH + O_2 + M \rightarrow CF_3CFHO_2 + M$	$k = 2.1 \times 10^{-12}$ cm^3 s^{-1} 14
4. $H + O_2 + M \rightarrow HO_2 + M$	$k = 5.9 \times 10^{-32}$ cm^6 s^{-1} 15
5. $HO_2 + HO_2 \rightarrow H_2O_2 + O_2$	$k = 2.8 \times 10^{-13} e^{594/T}$ cm^3 s^{-1} 9,16
6a. $CF_3CFHO_2 + CF_3CFHO_2 \rightarrow 2CF_3CFHO + O_2$	$k = 6.6 \times 10^{-13} e^{605/T}$ cm^3 s^{-1} 7
6b. $CF_3CFHO_2 + CF_3CFHO_2 \rightarrow CF_3C(O)F + CF_3CFHOH + O_2$	$k = 1.2 \times 10^{-13} e^{605/T}$ cm^3 s^{-1} 7
7. $CF_3CFHO_2 + HO_2 \rightarrow CF_3CFHOOH + O_2$	$k = 1.8 \times 10^{-13} e^{910/T}$ cm^3 s^{-1} [b]
8. $CF_3CFHO \rightarrow CF_3 + HC(O)F$	$k = 3.7 \times 10^{7} e^{-2200/T}$ s^{-1} 7
9. $CF_3 + O_2 + M \rightarrow CF_3O_2 + M$	$k = 6 \times 10^{-12}$ cm^3 s^{-1} 16
10. $CF_3CFHO_2 + CF_3O_2 \rightarrow CF_3CFHO + CF_3O + O_2$	$k = 8 \times 10^{-12}$ cm^3 s^{-1} 7
11. $CF_3O_2 + HO_2 \rightarrow CF_3OOH + O_2$	$k = k_7$
12. $CF_3O_2 + CF_3O_2 \rightarrow$ products	$k_{obs} = 3.1 \times 10^{-12}$ cm^3 s^{-1} 8
13. $CF_3CFHO_2 + CF_3CFHO \rightarrow$ products	$k = 5 \times 10^{-12}$ cm^3 s^{-1} ($\leq$240K)[7]
14. $HO_2 + CF_3CFHO \rightarrow$ products	$k = (0–2) \times 10^{-11}$ cm^3 s^{-1}

[a] Reaction numbers correspond to those used in the text. [b] Measured in the present study.

$$F + H_2 \rightarrow H + HF \quad (2)$$

$$CF_3CFH + O_2 + M \rightarrow CF_3CFHO_2 + M \quad (3)$$

$$H + O_2 + M \rightarrow HO_2 + M \quad (4)$$

The concentrations of CF_3CFH_2, H_2, and O_2 are chosen sufficiently large to ensure that these reactions are essentially complete and, thus, that the initial populations of CF_3CFHO_2 and HO_2 radicals are formed within a few microseconds of the photolysis pulse. This time is short compared to the subsequent peroxy radical reactions. A source of interference in these experiments arises from the formation of FO_2 via

$$F + O_2 + M \rightarrow FO_2 + M$$

This is due to the fact that FO_2 absorbs UV light in the same spectral region as the peroxy radicals, except with an intensity 3 times as large.[8] To avoid this interference, the ratio of $[CF_3CFH_2]/[O_2]$ is made large enough to limit FO_2 formation to a few percent of the total radical population.

F_2 photolysis is used to initiate the radical reactions for the kinetics measurements instead of the more conventional Cl_2 used for the product study. The reason is that the $Cl + CF_3CFH_2$ reaction has a rate constant 3 orders of magnitude smaller than that of reaction 1. It is desirable to form the reactants CF_3CFHO_2 and HO_2 on a time scale fast compared to their subsequent reactions. A 10 μs half-life for CF_3CFHO_2 formation would require flowing about 1400 Torr of CF_3CFH_2. Besides the obvious inconvenience in using this much precursor, it could introduce sufficient amounts of what would ordinarily be deemed "trace" impurities to interfere with the desired reactions.

The reaction mixture is probed by the broad-band light from a D_2 lamp which counterpropagates through the reaction cell and is dispersed by a 0.32 m monochromator and 147 groove/mm grating onto a gated, intensified, diode array detector. Time-resolved spectra are recorded at various delay times with respect to the photolysis pulse in the 10 μs–4 ms range with a temporal resolution of 20 μs for delays <200 μs and 40 μs for delays $\geq$200 μs. The absorbances of the reaction mixture are deconvoluted using the expression

$$\mathrm{Abs}(t) = [CF_3O_2 + HO_2]_t l\sigma(HO_2) + [CF_3CFHO_2]_t l\sigma(CF_3CFHO_2)$$

where l represents the path length and σ the wavelength dependent cross section of the particular peroxy radical and where the concentrations are treated as fitting parameters. Note that in the above expression the contributions to the total absorbance of the CF_3O_2 and HO_2 radicals are combined into a single term. CF_3O_2 is a degradation product of the CF_3CFHO_2 self-reaction

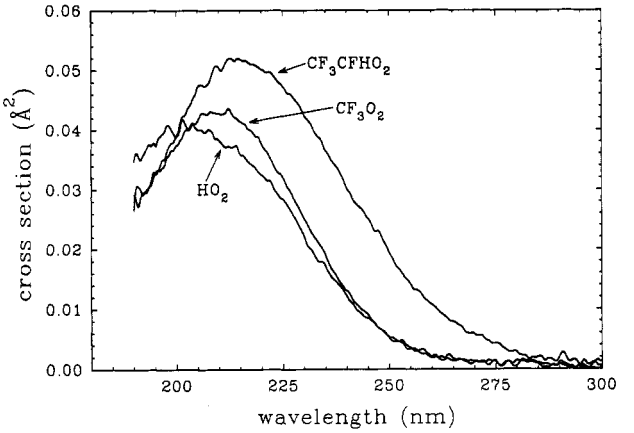

Figure 1. A comparison of the UV absorption spectra of CF_3CFHO_2, (ref 7), CF_3O_2 (ref 8), and HO_2 (ref 9).

(see reaction mechanism in Table 1). The reason for combining the two species is that the UV absorption spectra of CF_3O_2 (ref 8) and HO_2 (ref 9) are nearly identical both in absolute magnitude and in shape, as illustrated by Figure 1 (also shown is the spectrum of CF_3CFHO_2 (ref 7)). As as result, it is not possible to separate their individual contributions to the total absorbance (*vide infra*). Our measurements show $CF_3C(O)F$ to have a peak UV absorption of 2.8×10^{-20} cm^2 at 212 nm, a value negligble to the peroxy radical cross sections. Likewise, the HC(O)F product of HFC-134a degradation is expected, by analogy to CH_2O and CF_2O (ref 15), to contribute negligibly to the UV spectra. In contrast, the $CF_3CFHOOH$ product of the title reaction has an estimated absorption intensity in the 200 nm region roughly 1/10 that of the peroxy radicals (see section IIIa).

Temperature control is achieved using a Neslab ULT-80dd recirculating chiller which can be set between 210 and 363 K. The gases were precooled to a value within 10 K of the set point before entering the cell. Gas flow rates were regulated by Tylan flow controllers, except for F_2, for which the flow was set by a needle valve. The individual gas concentrations were determined by timing their flows into a constant volume and equating the partial pressure to the corresponding fractional flow times the total pressure. A typical gas mixture consisted of 6–12 Torr of H_2, 70–81 Torr of CF_3CFH_2, 35 Torr of 10% F_2/N_2, 75 Torr of O_2, and sufficient N_2 to achieve a total pressure of about 200 Torr.

B. FTIR Product Study. The experimental setup used for the present work has been described previously[10] and is only briefly discussed here. The apparatus consists of a Mattson Instruments Inc. Sirius 100 FT-IR spectrometer interfaced to a 140 L, 2 m long evacuable Pyrex chamber. White type multiple reflection optics were mounted in the reaction chamber to provide a total path length of 27 m for the IR analysis beam. The spectrometer

was operated at a resolution of 0.25 cm^{-1}. Infrared spectra were derived from 32 coadded interferograms.

CF_3CFHO_2 and HO_2 radicals were generated by the chlorine-initiated oxidation of mixtures of HFC-134a and H_2 in the presence of 10–147 Torr of O_2 at 700 Torr total pressure of N_2 diluent. Chlorine atoms were generated by the photolysis of molecular chlorine using the output of 22 UV fluorescent lamps (GTE F40BLB). CF_3CFHO_2 and HO_2 radicals are formed by the following reactions,

$$Cl_2 + h\nu\ (\lambda > 300\ nm) \rightarrow 2Cl$$

$$Cl + CF_3CFH_2\ (HFC\text{-}134a) \rightarrow CF_3CFH + HCl$$

$$CF_3CFH + O_2 \rightarrow CF_3CFHO_2$$

$$Cl + H_2 \rightarrow HCl + H$$

$$H + O_2 + M \rightarrow HO_2 + M$$

Initial concentrations used were as follows: HFC-134a, 100–104 mTorr; Cl_2, 104–400 mTorr; H_2, 0–206 mTorr; O_2, 10–147 Torr; N_2 diluent to a total pressure of 700 Torr. The temperature was 296 ± 2 K.

Products were quantified by fitting reference spectra of the pure compounds to the observed product spectra using integrated absorption features. Reference spectra were obtained by expanding known volumes of the reference material into the long path length cell. Systematic uncertainties associated with quantitative analyses using these reference spectra are estimated to be <10% for $CF_3C(O)F$ and COF_2 and <15% for HC(O)F and $CF_3O_3CF_3$.

The fitting procedure was as follows. HFC-134a was first quantified and subtracted from the product spectra using characteristic absorption features over the wavelength region 800–1500 cm^{-1}. HC(O)F, $CF_3C(O)F$, COF_2, and $CF_3O_3CF_3$ were then identified and quantified using features over the following wavelength ranges: 1700–1900, 1000–1200 and 1800–2000, 700–800 and 1800–2000, and 700–900 and 1100–1400 cm^{-1}, respectively. HFC-134a, Cl_2, $CF_3C(O)F$, and COF_2 were purchased from commercial vendors at purities ≥99%. HC(O)F was prepared from the reaction of benzoyl chloride with dry formic acid and anhydrous potassium fluoride.[11] $CF_3O_3CF_3$ was prepared by the UV irradiation of CF_3H–F_2–O_2–He mixtures.[12]

III. Results

A. HO_2 + CF_3CFHO_2 Kinetics. Photolysis of molecular fluorine in a mixture of CF_3CFH_2, H_2 and O_2 produces via reactions 1–4 initial populations of the peroxy radicals CF_3CFHO_2 and HO_2. The ratio of these radicals and the rate at which they are formed are controlled by the concentrations of CF_3CFH_2 and H_2 employed in the gas mixture. By using suitably large precursor and O_2 gas densities, the rates of peroxy radical formation can be made fast compared to their removal rates. Thus, the UV absorption spectrum of the reaction mixture immediately following the photolysis pulse (see Figure 2) should be a linear combination of the CF_3CFHO_2 and HO_2 spectra shown in Figure 1, weighted by their respective initial concentrations.

The peroxy radicals are expected to decay subsequently via the primary reactions

$$HO_2 + HO_2 \rightarrow HOOH + O_2 \quad (5)$$

$$CF_3CFHO_2 + CF_3CFHO_2 \rightarrow 2CF_3CFHO + O_2 \quad (6a)$$

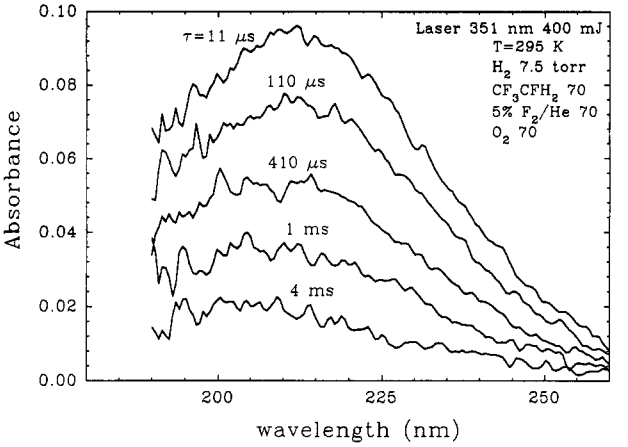

Figure 2. Time-resolved UV spectra of a $F_2/H_2/CF_3CFH_2/O_2/N_2$ gas mixture at various times following flash photolysis of the F_2.

$$CF_3CFHO_2 + CF_3CFHO_2 \rightarrow CF_3CFHOH + CF_3C(O)F + O_2 \quad (6b)$$

$$CF_3CFHO_2 + HO_2 \rightarrow CF_3CFHOOH + O_2 \quad (7a)$$

$$CF_3CFHO_2 + HO_2 \rightarrow CF_3C(O)F + H_2O + O_2 \quad (7b)$$

The disappearance of the peroxy radicals implies a decrease in the absorbance of the reaction mixture with increasing time, as observed in Figure 2. Since the CF_3CFHO_2 self-reaction rate constant is approximately 2.5 times larger than that of HO_2 (see Table 1), one expects, and observes in Figure 2, a concomitant shift of the absorption spectrum to the blue, reflecting the progressively larger fraction of HO_2 remaining in the reaction mixture.

Deconvolution of the time-resolved spectra, via the method described in section II, yields concentration versus time profiles for CF_3CFHO_2 and, nominally, HO_2, such as those illustrated in Figure 3. A challenge presented by this data is to fit simultaneously the decays of the two peroxy radicals using a single parameter, namely k_7. In the absence of complications arising from secondary chemistry, the $HO_2 + CF_3CFHO_2$ reaction rate constant would be deduced from fitting these data to predictions derived from a kinetic model corresponding to reactions 5–7 and the previously determined CF_3CFHO_2 and HO_2 self-reaction rate constants.[7,9] While this model can adequately fit the decay of CF_3CFHO_2, it significantly overestimates the apparent decay in HO_2 (Figure 3, filled circles versus dashed line).

The discrepancy originates from secondary chemistry of the alkoxy radical produced by the CF_3CFHO_2 self-reaction (reaction 6a). Several studies[17–21] have shown that under atmospheric conditions there is a competition between the two channels

$$CF_3CFHO \rightarrow CF_3 + HC(O)F \quad (8)$$

$$CF_3CFHO + O_2 \rightarrow CF_3C(O)F + HO_2$$

for removal of the alkoxy radical. At low O_2 partial pressures, such as employed in the present study, unimolecular decay is the primary channel.[7] In the presence of O_2 the CF_3 product is rapidly converted to the corresponding peroxy radical:

$$CF_3 + O_2 + M \rightarrow CF_3O_2 + M \quad (9)$$

As shown by Figure 1, CF_3O_2 exhibits a UV spectrum very similar to that of HO_2 in both shape and intensity. The similarity is sufficiently great that it is not feasible to distinguish the contribution of CF_3O_2 to the time-resolved absorbance of the

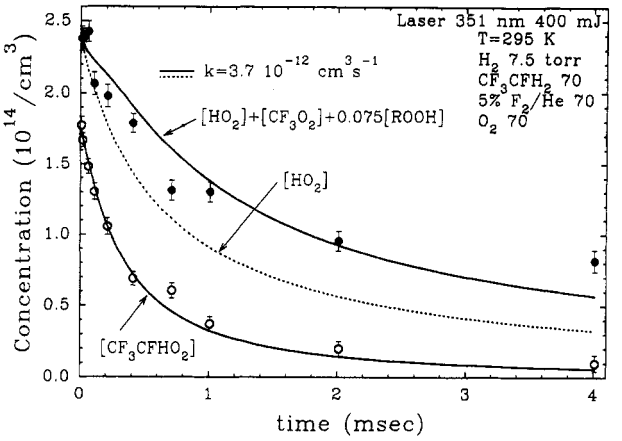

Figure 3. Concentration versus time profiles for HO_2 and CF_3CFHO_2 obtained by deconvolution of the corresponding time-resolved UV spectra. Solid and dashed lines show predictions from the model of Table 1.

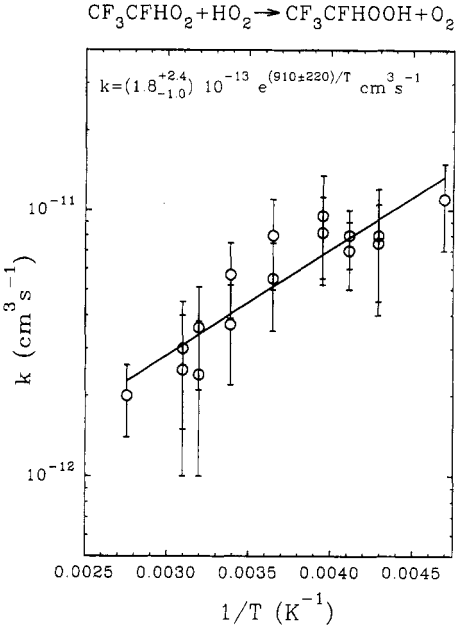

Figure 4. Rate constant versus temperature for the reaction $CF_3CFHO_2 + HO_2$.

reaction mixture from that of HO_2. Consequently, it appears that the HO_2 decays more slowly than expected because it is effectively replaced by CF_3O_2 produced via reactions 6a, 8, and 9. There is a second, analogous but smaller, effect due to $CF_3CFHOOH$ formed by reaction 7 and HOOH from reaction 5 (also less importantly CF_3OOH from reaction 11 in Table 1). The alkyl hydroperoxide molecules are assumed to have UV spectra similar to that of CH_3OOH. Both HOOH and CH_3OOH have spectra similar to the spectrum of HO_2 in the 200–250 nm region, but with absorption cross sections smaller by factors of 0.08 and 0.07, respectively, than that of HO_2 at 210 nm.[15] As can be seen from Figure 3, the predicted time dependence for the sum of the HO_2, CF_3O_2, and the ROOH (scaled by 0.075) concentrations is in reasonable agreement with the data. More importantly, it is possible to fit simultaneously the CF_3CFHO_2 decay and the composite HO_2, CF_3O_2, and ROOH decay with a single value for k_7.

Temperature-dependent rate constants for the title reaction are collected in Table 2 and shown in Figure 4. The rate constants were determined by fitting the $[CF_3CFHO_2]$ and the $[HO_2] + [CF_3O_2] + 0.075[ROOH]$ data simultaneously to the reaction model given in Table 1 with k_7 as the sole variational parameter. Rate constants for the other reactions have been previously reported, as indicated in the table, with the exception of reactions 11 and 14. These are included primarily for completeness; both have only minor effects on the fit for k_7. $HO_2 + RO_2$ reaction rate constants show relatively small variations for various R groups. The rate constants are typically in the range (5–20) × 10^{-12} cm^3 s^{-1} at 295 K, with a positive correlation between the size of the R group and the magnitude of the rate constant. Here we assume that $k_{11} \sim k_7$. The rate constant for reaction 14 was varied between 0 and 2 × 10^{-11} cm^3 s^{-1} and was found only to affect the $[HO_2] + [CF_3O_2] + 0.075[ROOH]$ composite predictions at low temperatures.

The least-squares fits were weighted by $1.0/[CF_3CFHO_2]_0$ and $0.5/[HO_2]_0$ for the CF_3CFHO_2 and composite data, respectively. The initial concentrations normalize the contributions from each data set to the least-squares sum. The weights of 1.0 versus 0.5 were chosen for two reasons: because the CF_3CFHO_2 predictions are more sensitive to changes in k_7 than those for $[HO_2] + [CF_3O_2] + 0.075[ROOH]$ and because they are subject to less uncertainty from secondary chemistry. The reported error bars (2σ errors of ±40% on average) originate from a statistical combination of fitting error (i.e., the sensitivity of the model predictions versus the scatter in the concentration versus time data), an error from the 10% uncertainty in the peroxy radical UV cross sections used to determine the radical concentrations, and uncertainties in the other rate constants used in the model (primarily k_5 and k_6). The majority of the error is due to fitting the concentration profiles, as reflected by the scatter in the data. This source of error is exacerbated in the present study because of the similarity between the spectra of the three

TABLE 2: F + CF_3CFH_2 and HO_2 + CF_3CFHO_2 Reaction Rate Constants

	conditions[a]					results[b]	
temp (K)	134a	H_2	O_2	total	$[F]_0$	$k_{F+CF_3CFH_2}$	$k_{HO_2+CF_3CFHO_2}$
210	70	5.9	70	219	5.3		11 ± 4
233	75	11	76	206	4.3	0.78 ± 0.13	7.5 ± 3
233	70	6.3	69	207	3.9	0.81 ± 0.14	8.0 ± 4
243	70	10	70	202	4.7	0.97 ± 0.15	8.0 ± 2
243	70	3.8	70	200	4.9	0.71 ± 0.14	7.0 ± 2
253	72	11	75	201	3.6	1.25 ± 0.21	8.2 ± 3
253	69	7.6	70	215	4.9	1.13 ± 0.19	9.5 ± 4
273	77	11	78	212	4.0	1.5 ± 0.26	5.5 ± 2
273	74	7.4	76	200	3.4	2.0 ± 0.34	8.0 ± 3
295	76	11	78	206	2.8	2.15 ± 0.37	5.7 ± 1.8
295	70	7.5	70	217	4.2	2.1 ± 0.37	3.7 ± 1.5
313	72	3.0	72	202	3.8	1.8 ± 0.27	2.4 ± 1.5
313	70	9.9	70	202	4.0	2.5 ± 0.38	3.6 ± 1.5
323	81	12	83	225	3.0	2.8 ± 0.48	3.0 ± 1.5
323	78	7.8	80	209	2.2	2.6 ± 0.44	2.5 ± 1.5
363	80	8.0	81	215	3.1	5.9 ± 1.0	2.0 ± 0.6

[a] Units are Torr, except for $[F]_0$ which is 10^{14} cm^{-3}. [b] Units are 10^{-12} cm^3 s^{-1}.

TABLE 3: Product Yields[a] (in percent) Following the Irradiation of HFC-134a/Cl_2/H_2/O_2 Mixtures in 700 Torr of N_2

expt no.	[HFC-134a]$_0$[b]	[Cl_2]$_0$	[H_2]$_0$	[O_2]$_0$	Δ[HFC-134a] (%)	$Y_{HC(O)F}$	Y_{CF_3COF}	$Y_{CF_3O_3CF_3}$	Y_{COF_2} balance	carbon
1	0.103	0.105	0	147	0–21	61 ± 6	23 ± 3	20 ± 3	29 ± 7	87 ± 13
2	0.104	0.104	0.022	147	0–19	63 ± 3	22 ± 2	7 ± 3	49 ± 9	85 ± 11
3	0.103	0.108	0.042	147	0–20	64 ± 4	22 ± 1	4 ± 2	55 ± 3	86 ± 7
4	0.101	0.107	0.102	147	0–19	57 ± 2	21 ± 2	≈1	52 ± 5	77 ± 7
5	0.102	0.203	0.206	147	0–21	57 ± 2	20 ± 2	≈1	53 ± 5	76 ± 6
6	0.101	0.106	0	10	0–20	71 ± 6	11 ± 4	32 ± 6	22 ± 4	90 ± 15
7	0.100	0.400	0.200	10	0–24	65 ± 9	9 ± 2	13 ± 2	67 ± 7	88 ± 12

[a] Molar yields defined as moles of product formed per mole of HFC-134a consumed. [b] All concentrations in Torr.

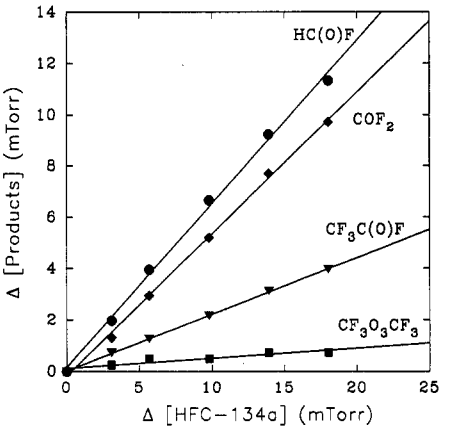

Figure 5. Observed concentrations of HC(O)F (●), COF_2 (◆), $CF_3C(O)F$ (▼), and $CF_3O_3CF_3$ (■) as a function of the loss of HFC-134a in experiment 3 (see Table 3).

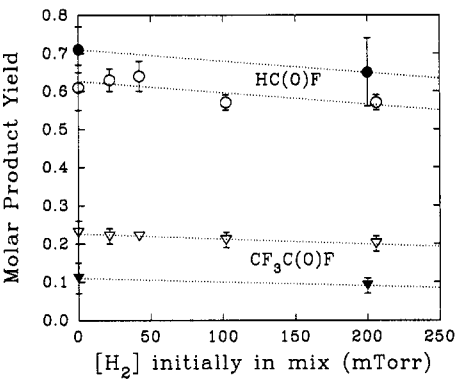

Figure 6. Observed yields of HC(O)F (circles) and $CF_3C(O)F$ (triangles) following the irradiation of mixtures of 0.1 Torr of HFC-134a, 0.1–0.4 Torr of Cl_2, 10 (filled symbols) or 147 (open symbols) Torr of O_2, and 0–0.2 Torr of H_2 as a function of the initial H_2 concentration present in the mix. The dotted lines are linear regressions to aid in visual inspection of the data.

peroxy radicals monitored by the time-resolved UV spectroscopy. It is worth noting that the error bars derived by the above analysis are consistent with the data scatter.

The temperature-dependent rate constants for the CF_3CFHO_2 + HO_2 reaction are well fit by an Arrhenius expression employing a negative activation energy, with the result that $k_7 = (1.8^{+2.4}_{-1.0}) \times 10^{-13} e^{(910\pm220)/T}$ cm^3 s^{-1}. The activation energy of E_a = −910 K lies intermediate between the values[4,3] of −790 K for CH_3O_2 and −1250 K for c-$C_6H_{11}O_2$, representing peroxy radicals with moderate and steep temperature dependences, respectively. However, the magnitudes of the rate constants are approximately two-thirds of those for the CH_3O_2 + HO_2 reaction, making the CF_3CFHO_2 + HO_2 reaction among the slowest of its class. The average room temperature rate constant of 4.7×10^{-12} cm^3 s^{-1} (the measured value as compared to 3.9×10^{-12} cm^3 s^{-1} from the best fit Arrhenius expression) is in good agreement with the value of 4×10^{-12} cm^3 s^{-1} reported by Hayman.[5]

B. Product Study. Seven experiments were performed as part of the present work. Each experiment consisted of a series of five successive 2–5 min irradiations of a HFC-134a/H_2/Cl_2/O_2/N_2 mixture. After each irradiation period the composition of the gas mixture was analyzed using FTIR spectroscopy. Four carbon-containing products were observed: HC(O)F, $CF_3C(O)F$, $CF_3O_3CF_3$, and COF_2. Results from all seven experiments are given in Table 3. Figure 5 shows the observed product formation as a function of the loss of HFC-134a following the irradiation of a mixture of 0.103 Torr of HFC-134a, 0.108 Torr of Cl_2, and 0.042 Torr of H_2, in 700 Torr of air diluent (experiment 3 in Table 3). The lines through the data in Figure 5 are linear least-squares fits which give the following molar yields: $Y_{HC(O)F}$ = 64 ± 4%, Y_{CF_3COF} = 22 ± 1%, $Y_{CF_3O_3CF_3}$ = 4 ± 2%, and Y_{COF_2} = 55 ± 3%. Quoted errors are two standard deviations.

As with all product studies, careful consideration needs to be given to the possibility of secondary reactions leading to product loss. In all experiments, plots of the formation of product versus loss of HFC-134a were linear with intercepts which were indistinguishable from the origin. Such behavior suggests, but does not prove, the absence of significant complicating secondary reactions. Unwanted secondary processes include photolysis, reaction with Cl atoms, and heterogeneous losses in the chamber. Previous studies in our laboratory have established that photolysis and heterogeneous loss of HC(O)F, $CF_3C(O)F$, $CF_3O_3CF_3$, and COF_2 are unimportant. Cl atoms do not react with $CF_3C(O)F$, $CF_3O_3CF_3$, and COF_2, and react only slowly with HC(O)F.[17]

There are two interesting points to note from the data given in Table 3. First, as shown in Figure 6, the yields of HC(O)F and $CF_3C(O)F$ are, within the experimental uncertainties, unaffected by the addition of H_2 (and hence HO_2 radicals) to the reaction mixtures. However, addition of H_2 causes a decrease in the $CF_3O_3CF_3$ yield and an increase in the COF_2 yield (see Table 3). Second, the observed products account for most, but not all, of the HFC-134a loss. Approximately 10–20% of the HFC-134a loss is unaccounted for. There appears to be a small drop in the carbon balance on addition of H_2, but the drop is well within the experimental uncertainties.

The mechanism of the Cl atom initiated oxidation of HFC-134a has been studied extensively in our laboratory[17,22,23] and is well described by the reactions given in Table 4. The principal reactions in this mechanism are identical to those in Table 1. Two mechanisms are provided for convenience. They differ in two respects: First, Cl atoms are used to initiate the reaction sequence in the product study as opposed to F atoms in the kinetic measurements. Second, a larger number of secondary reactions are needed to model the product study as compared to the kinetic study. The expected products are HC(O)F, $CF_3C(O)F$, $CF_3O_3CF_3$, COF_2, CF_3OH, and $CF_3O_3CFHCF_3$. The latter two products undergo rapid decomposition in the reaction chamber[22] and were not detected in the present work.

It is striking that the addition of H_2 to reaction mixtures containing HFC-134a and Cl_2 in air diluent does not affect the yield of HC(O)F or $CF_3C(O)F$. For example, compare experiments 1 and 3 in Table 3. In the presence of H_2 reactions 15 and 16 compete for the available Cl atoms.

$$Cl + CF_3CFH_2\ (HFC\text{-}134a) \rightarrow CF_3CFH + HCl \qquad (15)$$

TABLE 4: Reaction Mechanism

reaction	k(296 K)[a]	ref/comments
$Cl_2 \rightarrow 2Cl$		
HFC Chemistry		
$Cl + CF_3CFH_2 \rightarrow HCl + CF_3CFH$	1.4×10^{-15}	22
$CF_3CFH + O_2 \rightarrow CF_3CFHO_2$	2.1×10^{-12}	14
$CF_3CFHO_2 + CF_3CFHO_2 \rightarrow 2CF_3CFHO + O_2$	5.1×10^{-12}	7
$CF_3CFHO_2 + CF_3CFHO_2 \rightarrow CF_3C(O)F + CF_3CFHOH + O_2$	9.3×10^{-13}	7
$CF_3CFHO_2 + CF_3O_2 \rightarrow CF_3CFHO + CF_3O + O_2$	8×10^{-12}	7
$CF_3CFHO \rightarrow CF_3 + HC(O)F$	2.2×10^{4}	7
$CF_3CFHO + O_2 \rightarrow CF_3C(O)F + HO_2$	9×10^{-16}	22
$CF_3 + O_2 \rightarrow CF_3O_2$	8.5×10^{-12}	16
$CF_3O_2 + CF_3O_2 \rightarrow CF_3O + CF_3O + O_2$	1.8×10^{-12}	8, 22
$CF_3O + CF_3O_2 \rightarrow CF_3O_3CF_3$	2.5×10^{-11}	8, 22
$CF_3O + CF_3CFHO_2 \rightarrow CF_3CFHO_3CF_3$	1.8×10^{-11}	22
$CF_3CFHO_3CF_3 \rightarrow CF_3CFHO_2 + CF_3O$	2.0×10^{-3}	22
$CF_3CFHO_3CF_3 \rightarrow CF_3CFHO + CF_3O_2$	2.0×10^{-3}	22
$CF_3O + CF_3CFH_2 \rightarrow CF_3CFH + CF_3OH$	4.5×10^{-16}	22
$CF_3OH \rightarrow COF_2 + HF$	1×10^{-2}	23
$Cl + HC(O)F \rightarrow HCl + FCO$	2.0×10^{-15}	22
HO_2 Chemistry		
$Cl + H_2 \rightarrow HCl + H$	1.6×10^{-14}	15
$H + O_2 + M \rightarrow HO_2 + M$	1.1×10^{-12}	15
$HO_2 + HO_2 \rightarrow H_2O_2 + O_2$	2.8×10^{-12}	15
$HO_2 + CF_3CFHO_2 \rightarrow CF_3CFHOOH + O_2$	3.9×10^{-12}	this work
$Cl + CF_3CFHOOH \rightarrow CF_3CFHO_2 + HCl$	1.5×10^{-13}	*b*
$HO_2 + CF_3O_2 \rightarrow CF_3OOH + O_2$	3.9×10^{-12}	*c*
$Cl + CF_3OOH \rightarrow CF_3O_2 + HCl$	1.5×10^{-13}	*b*
$Cl + H_2O_2 \rightarrow HO_2 + HCl$	4.1×10^{-13}	15

[a] Units of $cm^3\ s^{-1}$. [b] Assumed equal to $k(Cl+CH_2FOOH)$ [ref 26]. [c] Assumed equal to $k(HO_2+CF_3CFHO_2)$.

$$Cl + H_2 \rightarrow HCl + H \quad (16)$$

The rate constant ratio is[15,24] $k_{16}/k_{15} = 1.6 \times 10^{-14}/1.4 \times 10^{-15} = 11$. In experiment 3 the concentration ratio is $[H_2]_0/[HFC\text{-}134a]_0 = 0.4$. Hence, the initial rate of HO_2 radical production is 5 times that of CF_3CFHO_2 radicals. Despite the fact that an excess of HO_2 radicals are produced during experiment 3, their presence has little, or no, effect on the observed yields of HC(O)F and $CF_3C(O)F$.

There is only one source of HC(O)F in the present chemical system: unimolecular decomposition of the alkoxy radical CF_3CFHO.

$$CF_3CFHO \rightarrow CF_3 + HC(O)F$$

The alkoxy radical CF_3CFHO is produced in a yield of 84–95% following the self-reaction of CF_3CFHO_2 radicals,[17,18,21] There are two possible explanations of the insensitivity of the HC(O)F yield to the presence of H_2 in the reaction mixtures. Either HO_2 radicals do not react significantly with CF_3CFHO_2 radicals under the experimental conditions, or there is a reaction but the product(s) are directly, or indirectly, converted into CF_3CFHO radicals in a yield of approximately 84%.

The rate constant for reaction 7, $CF_3CFHO_2 + HO_2 \rightarrow$ products, has been measured as part of this work. With $k_7 = 3.9 \times 10^{-12}\ cm^3\ s^{-1}$ and the chemical mechanism given in Table 4, we can estimate the importance of reaction 7 as a loss process for CF_3CFHO_2 radicals. Using the Acuchem chemical kinetic modeling program,[25] reaction 7 is predicted to account for 32% of the loss of CF_3CFHO_2 radicals in experiment 3 and 80% in experiment 5. Clearly, reaction 7 is an important fate of CF_3CFHO_2 radicals. By analogy to the existing data base concerning the reaction of organic peroxy radicals[26] with HO_2, reaction 7 is expected to yield either a hydroperoxide, or carbonyl product, or both.

$$CF_3CFHO_2 + HO_2 \rightarrow CF_3CFHOOH + O_2 \quad (7a)$$

$$CF_3CFHO_2 + HO_2 \rightarrow CF_3C(O)F + H_2O + O_2 \quad (7b)$$

The carbonyl product, $CF_3C(O)F$, does not react with Cl atoms, nor is it lost via photolysis or heterogeneous processes in the chamber. If $CF_3C(O)F$ were a major product of reaction 7, the yield of $CF_3C(O)F$ should increase on addition of H_2 to the reaction mixtures. The increase in $CF_3C(O)F$ should be particularly evident for experiment 7 where the O_2 partial pressure was only 10 Torr and the yield of $CF_3C(O)F$ via reaction of the alkoxy radical CF_3CFHO with O_2 was suppressed. As seen from Figure 6, there was no discernible increase in the $CF_3C(O)F$ yield on addition of H_2, suggesting that channel 7b is of minor importance.

Channel 7a gives the a hydroperoxide, $CF_3CFHOOH$. Since this compound is unavailable commercially, we have not been able to establish its behavior in the chamber with regard to reaction with Cl atoms, photolysis, and possible heterogeneous loss. None of the hydroperoxides investigated thus far in our chamber (CH_3OOH, C_2H_5OOH, cyclo-C_5H_9OOH, cyclo-$C_6H_{11}OOH$, CH_2FOOH, CH_2ClOOH) have shown any evidence of photolysis or heterogeneous decomposition.[26] It seems reasonable to suppose that $CF_3CFHOOH$ will not be lost via photolysis or heterogeneous decomposition either. Hydroperoxides do react with Cl atoms. The rate constant for the reaction of Cl atoms with monofluoromethyl hydroperoxide, CH_2FOOH, is $(1.5 \pm 0.5) \times 10^{-13}\ cm^3\ s^{-1}$, with the reaction proceeding via attack on the OO–H group.[26] It is interesting to note that H_2O_2 which has two OO–H sites reacts with Cl atoms with a rate[15] ($4.1 \times 10^{-13}\ cm^3\ s^{-1}$) which is twice that observed for CH_2FOOH. We make the reasonable assumption that the rate constant for the attack of a Cl atom on the OO–H group of $CF_3CFHOOH$ is the same as for CH_2FOOH, $\approx 1.5 \times 10^{-13}\ cm^3\ s^{-1}$. The rate constant for the reaction of Cl atoms with $CF_3CFHOOH$ is then 2 orders of magnitude greater than that for the reaction of Cl atoms with HFC-134a ($1.4 \times 10^{-15}\ cm^3\ s^{-1}$).[24,27] For the experimental conditions given in Table 3 the consumption of HFC-134a is 19–24%, and any $CF_3CFHOOH$ product will be rapidly consumed by Cl atom attack.

$$Cl + CF_3CFHOOH \rightarrow CF_3CFHO_2 + HCl \quad (17)$$

Reaction 17 regenerates CF_3CFHO_2 radicals and masks the effect of reaction 7a. To explore the effect of reaction 17 on the yields

of HC(O)F and $CF_3C(O)F$, this reaction was added to the mechanism given in Table 4. Simulations using this mechanism showed that for the experimental conditions given in Table 3 reaction 17 suppresses the concentration of $CF_3CFHOOH$ to a level below the experimental detection limit of 1–2 mTorr for hydroperoxides (using the characteristic OO–H stretching frequency around 3600 cm^{-1}). Consistent with the experimental observations, the mechanism in Table 4, which includes reaction 17, predicts that the yields of HC(O)F and $CF_3C(O)F$ should be unaffected by the presence of H_2 in the reaction mixtures.

As seen in Table 3, and noted above, the addition of H_2 to the reaction mixtures causes a decrease in the yield of the trioxide, $CF_3O_3CF_3$ and an increase in the yield of COF_2. The only source of COF_2 is the present experiments is the decomposition of CF_3OH, which is a product of the reaction of CF_3O with hydrogen-containing species. With the addition of H_2 to the reaction mixtures more H-containing species are available for the CF_3O radicals to react with. Thus, an increase in COF_2 yield on addition of H_2 is not unexpected. The trioxide $CF_3O_3CF_3$ is formed by the combination of CF_3O and CF_3O_2 radicals. The presence of additional loss mechanisms for CF_3O radicals in those experiments where H_2 is added explains the experimentally observed decrease in $CF_3O_3CF_3$ yield. In the mechanism given in Table 4, for every HC(O)F molecule formed a CF_3 radical is generated. The CF_3 radicals are then transformed into either COF_2 (via CF_3OH) or $CF_3O_3CF_3$. It follows that the yield of HC(O)F should equal the sum of the COF_2 yield and twice the $CF_3O_3CF_3$ yield. Within the experimental uncertainties, this was the case in all experiments. Finally, we need to consider the carbon balance. The observed carbon-containing products accounted for 77–90% of the HFC-134a loss. The self-reaction of CF_3CFHO_2 radicals is believed to proceed to give the alcohol, CF_3CFHOH, in 5–8% yield.[17,18,21] This compound was not detected in the present work, consistent with its small yield. It might be expected then that the carbon balance would approach 92–95%, and with the exception of experiments 4 and 5, this is indeed the case. For experiments 4 and 5 the carbon balance is approximately 10% less than in the other experiments; the cause of this is unclear. CF_3CFHOH may react with Cl atoms and be converted into $CF_3C(O)F$. At the present time there is no available kinetic data for such a reaction; thus, it is not possible to assess its potential importance.

The results from the present work show that $CF_3C(O)F$ is a minor product of the reaction between CF_3CFHO_2 and HO_2 radicals, and by inference, $CF_3CFHOOH$ is the dominant product. To establish an upper limit for the importance of reaction channel 7b this reaction was added to the mechanism in Table 4, and simulations of experiments 6 and 7 were performed. The $CF_3C(O)F$ yield in experiment 6 could be as low as 7% while that in experiment 7 could be as high as 11%. From simulations using the chemical mechanism in Table 4, it was found that $k_{7b}/(k_{7a} + k_{7b})$ must be ≤ 0.05 for the $CF_3C(O)F$ yield to increase by no more than 4% in the presence of 0.2 Torr of H_2. By inference, $k_{7a}/(k_{7a} + k_{7b}) \geq 0.95$.

In the experiments described thus far no direct evidence for the formation of the hydroperoxide $CF_3CFHOOH$ was observed. As discussed above, the absence of $CF_3CFHOOH$ is attributed to the rapid removal of this species by secondary reaction with Cl atoms. To minimize such secondary reactions, small (<1%) fractional conversions of HFC-134a must be used. This, in turn, requires a large (>1 Torr) initial concentration of HFC-134a. As the initial HFC-134a concentration is increased above approximately 0.2 Torr, the HFC-134a absorption features become optically black and obscure large regions of the spectrum. Fortunately, HFC-134a does not absorb significantly in the region 3500–3700 cm^{-1} where the OO–H stretch is expected and 700–800 cm^{-1} where a characteristic $CF_3C(O)F$ feature is located. Two experiments were performed using mixtures of 10.2 Torr of HFC-134a and 0.3–0.5 Torr of Cl_2 in 700 Torr total pressure of O_2 diluent with, and without, 2.13 Torr of H_2. In both experiments a product was observed with a broad absorption feature in the region 3550–3600 cm^{-1} characteristic of the OO–H stretch in hydroperoxides. The yield of the hydroperoxide was estimated by comparing the integrated absorption over the range 3550–3600 cm^{-1} with that of a calibrated spectrum of ethyl hydroperoxide as described previously.[28] In the experiment without H_2 the ratio of the yield of $CF_3C(O)F$ to hydroperoxide after 2 min irradiation was 48 mTorr/10.4 mTorr = 4.6. In the experiment with H_2 present, 60 s of irradiation gave a product mixture in which the ratio of the yield of $CF_3C(O)F$ to hydroperoxide was 18 mTorr/9.3 mTorr = 1.9. Simulation of these experiments using the mechanism given in Table 4 predicts product ratios of 3.8 and 2.0 for $CF_3CFHOOH/CF_3C(O)F$ in the absence and presence of H_2, respectively. The fact that the simulated results are, within the experimental uncertainties, consistent with those observed experimentally supports (but does not prove) the notion that reaction of CF_3CFHO_2 radicals with HO_2 produces the hydroperoxide $CF_3CFHOOH$.

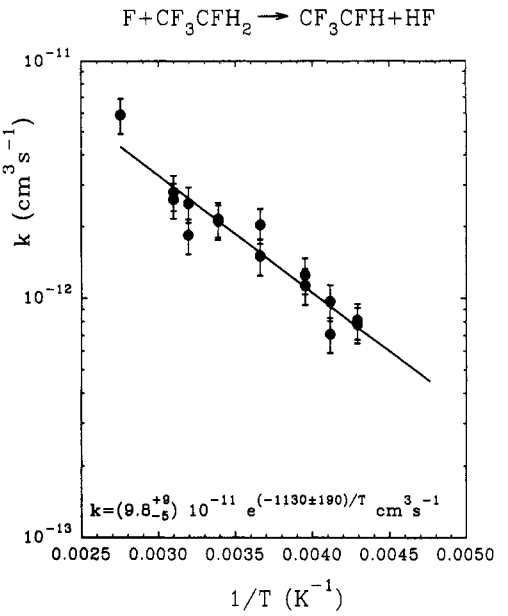

Figure 7. Rate constant versus temperature for the reaction F + CF_3CFH_2.

C. F + CF_3CFH_2. A competition between fluorine attack of CF_3CFH_2 versus H_2 was used to establish the initial peroxy radical concentrations for the CF_3CFHO_2 reaction discussed in section IIIA. This competition affords the opportunity to measure k_1 relative to k_2; thus,

$$\frac{k_1}{k_2} = \frac{[CF_3CFHO_2]_0[H_2]}{[HO_2]_0[CF_3CFH_2]}$$

assuming that the O_2 addition reactions are essentially instantaneous. Using the literature value[13] of $k_2 = 1.7 \times 10^{-10} e^{-550/T}$ cm^3 s^{-1} provides the F + CF_3CFH_2 rate constants listed in Table 2 and illustrated in Figure 7. Our results can be compared to room temperature values for k_1 measured by Wallington et al.[29] by a variety of techniques. One method gives a rate constant of $(2.1 \pm 0.7) \times 10^{-12}$ cm^3 s^{-1} relative to F + O_2, which is in good agreement with the present value of $k_1 = (2.1 \pm 0.4) \times 10^{-12}$ cm^3 s^{-1} at 295 K measured relative to F + H_2. Two other techniques yield somewhat smaller values of $(1.4 \pm 0.3) \times 10^{-12}$ cm^3 s^{-1} relative to F + O_2 and $(1.3 \pm 0.3) \times 10^{-12}$ cm^3 s^{-1} relative (via intermediate steps) to F + CH_4.[29] The discrepancy with the latter measurements could, at least partly, be due to uncertainties in the rate constants for the reference reactions.

As expected for a hydrogen abstraction reaction, the rate constants follow Arrhenius behavior (see Figure 7). A least-

squares fit of the data reveals that $k_1 = (9.8^{+9}_{-5}) \times 10^{-11}$ $e^{(-1130\pm190)/T}$ cm^3 s^{-1}. For comparison, the activation energy of $E_a = 1130$ K is about 3 times larger than the E_a for the fluorine plus ethane reaction, whereas the A factor is 7 times smaller.[9] The higher activation energy is consistent with previous observations that fluorine substitution of alkanes increases the C–H bond energy of the remaining hydrogen atoms.[30,31]

IV. Atmospheric Implications

The predominant eventual atmospheric fate of alkylperoxy radicals is their conversion to the corresponding alkoxy radical. The reactions of RO_2 with NO and $R'O_2$ accomplish this directly, whereas the reactions with HO_2 and NO_2 temporarily sequester the peroxy radical in the forms ROOH and RO_2NO_2, respectively. With respect to the degradation of HFC-134a, the alkoxy radical either dissociates into CF_3 and HC(O)F or reacts with O_2 to form $CF_3C(O)F$ and HO_2, with a branching ratio that depends on temperature, oxygen concentration, and total pressure. Potentially, the reaction between CF_3CFHO_2 and HO_2 could "short circuit" the formation of HC(O)F, if channel 7b were important, resulting in a higher ratio of $CF_3C(O)F$ to HC(O)F production. However, the FTIR product study shows this possibility to be at most a minor one.

The major product of the $CF_3CFHO_2 + HO_2$ reaction is $CF_3CFHOOH$. Atmospheric ROOH loss is expected to occur via photodissociation and reaction with hydroxyl radicals;[32] in the case of R = CF_3CFH these are

$$CF_3CFHOOH + h\nu \rightarrow CF_3CFHO + OH \quad (18)$$

$$CF_3CFHOOH + OH \rightarrow CF_3CFHO_2 + H_2O \quad (19)$$

Photolysis of the hydroperoxide yields the alkoxy radical, whereas the reaction with OH returns the initial peroxy radical. Thus, the net effect of the reaction between peroxy radical and HO_2 is to delay formation of the alkoxy radical, or in effect, to increase the atmospheric lifetime of the peroxy radical.

Neither the photodissociation cross section nor the rate constant for reaction with OH is known for $CF_3CFHOOH$. However, it is reasonable to assume that its UV spectrum is similar to that of CH_3OOH, which in turn is similar to that of HOOH, which has a photolysis rate ("J" value) on the order of 10^{-5} s^{-1}.[15] For comparison, the $CH_3OOH + OH$ reaction has an overall rate constant of $2.93 \times 10^{-2}e^{190/T}$ cm^3 s^{-1} and a 67% yield of CH_3O_2 at 298 K.[33] Assuming that the rate constant for reaction 19 is of the same magnitude and that the OH concentration[15] is approximately 10^6 cm^{-3} the rate for the removal of $CF_3CFHOOH$ by reaction with hydroxyl radicals is on the order of 5×10^{-6} s^{-1}, i.e., comparable to the photolysis rate. The atmospheric half-life of $CF_3CFHOOH$ is, therefore, approximately 1 day. In contrast, if we assume an NO concentration[15] of 5×10^8 cm^{-3} and take $k(CF_3CFHO_2+NO) = 1.3 \times 10^{-11}$ cm^3 s^{-1}, the half-life of CF_3CFHO_2 with respect to reaction with NO is a few minutes. Hence, the reaction with HO_2 can efficiently sequester the peroxy radical.

Whether or not the sequestering has an impact on the atmospheric degradation of HFC-134a depends on the relative concentration $[NO]/[HO_2]$ and on the relative value of the rate constants for CF_3CFHO_2 reaction with HO_2 versus NO. The concentration ratio varies with altitude and is expected to be higher over industrialized areas versus remote areas. The JPL compilation[15] gives $[NO]/[HO_2] \sim 4$ at 10 km altitude, while the Rural Oxidants in the Southern Environment study by Cantrell et al.[34] shows the ratio to be roughly 2 near ground level in the rural environment. At 295 K, $k(CF_3CFHO_2+NO)/k(CF_3CFHO_2+HO_2) \sim 3$, whereby approximately 10% of the CF_3CFHO_2 should be sequestered in the form of $CF_3CFHOOH$. However, the $HO_2 + CF_3CFHO_2$ reaction shows a moderately steep negative temperature dependence. While the temperature dependence of the reaction with NO is unknown, comparison to other $RO_2 + NO$ reactions[1,3,4] suggests that this reaction is relatively temperature independent. In this case, the rate constants become comparable in the colder regions of the atmosphere, and the fraction of CF_3CFHO_2 radicals reacting with HO_2 could approach 25%.

V. Conclusion

The reaction between CF_3CFHO_2 and HO_2 has been investigated over the 210–363 K temperature range using time-resolved UV spectroscopy. This technique allows the time-dependent concentrations of CF_3CFHO_2 and of $HO_2 + CF_3O_2 +$ 0.075ROOH to be extracted from the variation in time of the UV absorbance of a mixture of fluorine, HFC-134a, H_2, and O_2 following flash photolysis of the F_2. Individual concentration dependences for HO_2, CF_3O_2, and ROOH cannot be determined because the UV spectra of these species are too similar to each other. The CF_3CFHO_2 and $HO_2 + CF_3O_2 +$ 0.075ROOH concentrations are simultaneously fit to a reaction model with one unknown parameter, namely, the $CF_3CFHO_2 + O_2$ rate constant, and yield $k_7 = (1.8^{+2.4}_{-1.0}) \times 10^{-13}e^{(910\pm220)/T}$ cm^3 s^{-1}. The temperature dependence of this reaction is consistent with that of other known $RO_2 + HO_2$ reactions; however, the preexponential factor is smaller, making this one of the slowest reactions of its type.

The FTIR product study reveals that the formation of $CF_3C(O)F$ is unaffected by the addition of H_2 to the reaction mixture. This is consistent with <5% of the reaction between CF_3CFHO_2 and HO_2 proceeding via channel 7b and implies that >95% proceeds via channel 7a to form $CF_3CFHOOH$. The hydroperoxide reacts rapidly with Cl atoms to regenerate the peroxy radical, with the net result that the products are essentially the same as obtained from the CF_3CFHO_2 self-reaction. Under conditions of a large initial concentration of HFC-134a, the rate of $CF_3CFHOOH$ removal by Cl atoms is suppressed relative to its formation, and infrared features characteristic of the OOH group are observed at intensities consistent with reaction 7a as the principal channel.

Utilizing the competition between HFC-134a and H_2 for fluorine atoms, the initial CF_3CFHO_2 and HO_2 concentrations provide a relative rate constant for $F + CF_3CFH_2$ of $k_1 = (9.8^{+9}_{-5}) \times 10^{-11}$ $e^{(-1130\pm190)/T}$ cm^3 s^{-1}. The higher activation energy for this reaction as compared to that for ethane, for example, reflects an increase in C–H bond strength from fluorine substitution.

The rate constant for the reaction of CF_3CFHO_2 with HO_2 is about 3 times smaller than the rate constant for the reaction with NO at 295 K. Assuming a negligible temperature dependence for the NO reaction, the two rate constants become comparable at about 210 K. Combined with a $[NO]/[HO_2]$ ratio of approximately 3, this implies that 10–25% of the CF_3CFHO_2 radicals will be sequestered as $CF_3CFHOOH$ rather than be converted to CF_3CFHO via reaction with NO. Other than introducing a small delay into the degradation of the peroxy radical, the reaction with HO_2 is, therefore, expected to have a minor impact on the overall atmospheric degradation of HFC-134a.

References and Notes

(1) Francisco, J. S.; Maricq, M. M. *Adv. Photochem.*, in press.
(2) Wallington, T. J.; Nielsen, O. J. *Chem. Phys. Lett.* **1991**, *187*, 33.
(3) Wallington, T. J.; Dagaut, P.; Kurylo, M. J. *Chem. Rev.* **1992**, *92*, 667.
(4) Lightfoot, P. D.; Cox, R. A.; Crowley, J. N.; Destriau, M.; Hayman, G. D.; Jenkin, M. E., Moortgat, G. K.; Zabel, F. *Atmos. Environ.* **1992**, *26A*, 1805.
(5) Hayman, G. D. AFEAS Workshop on Atmospheric Degradation of HCFCs and HFCs, Boulder, CO, Nov 1993.
(6) Maricq, M. M.; Wallington, T. J. *J. Phys. Chem.* **1992**, *96*, 986.
(7) Maricq, M. M.; Szente, J. J. *J. Phys. Chem.* **1992**, *96*, 10862.
(8) Maricq, M. M.; Szente, J. J. *J. Phys. Chem.* **1992**, *96*, 4925.

(9) Maricq, M. M.; Szente, J. J. *J. Phys. Chem.* **1994**, *98*, 2078.
(10) Wallington, T. J.; Gierczak, C. A.; Ball, J. C.; Japar, S. M. *Int. J. Chem. Kinet.* **1989**, *21*, 1077.
(11) Morgan, H. W.; Staats, P. A.; Goldstein, J. H. *J. Chem. Phys.* **1956**, *25*, 337.
(12) Wallington, T. J.; Sehested, J.; Dearth, M. A.; Hurley, M. D. *J. Photochem. Photobiol., A: Chem.* **1993**, *70*, 5.
(13) Westley, F.; Herron, J. T.; Cvetanovic, R. J.; Hampson, R. F.; Mallard, W. G. NIST Chemical Kinetics Database, NIST, Gaithersburg, 1991.
(14) Maricq, M. M.; Szente, J. J.; Kaiser, E. W. *Chem. Phys. Lett.* **1992**, *197*, 149.
(15) DeMore, W. B.; Sander, S. P.; Golden, D. M.; Hampton, R. F.; Kurylo, M. J.; Howard, C. J.; Ravishankara, A. R.; Kolb, C. E.; Molina, M. J. Chemical Kinetics and Photochemical Data for Use in Stratospheric Modeling. JPL Publication 92–20, 1992.
(16) Atkinson, R.; Baulch, D. L.; Cox, R. A.; Hampson, R. F., Jr.; Kerr, J. A.; Troe, J. *J. Phys. Chem. Ref. Data* **1992**, *21*, 1125.
(17) Wallington, T. J.; Hurley, M. D.; Ball, J. C.; Kaiser, E. W. *Environ. Sci. Technol. 26*, 1992, 1318.
(18) Tuazon, E. C.; Atkinson, R. *J. Atmos. Chem.* **1993**, *16*, 301.
(19) Rattigan, O. V.; Rowley, D. M.; Wild, O.; Jones, R. L.; Cox, R. A. Proceedings of the STEP-HALOCSIDE/AFEAS Workshop, Dublin, 1993.
(20) Zellner, R.; Hoffmann, A.; Mörs, V.; Maims, W. Proceedings of the STEP-HALOCSIDE/AFEAS Workshop, Dublin, 1993.
(21) Meller, R.; Boglu, D.; Moortgat, G. K. proceedings of the STEP-HALOCSIDE/AFEAS Workshop, University College Dublin, Ireland, March 1993; p 130.
(22) Sehested, J.; Wallington, T. J. *Environ. Sci. Technol.* **1993**, *27*, 146.
(23) Wallington, T. J.; Hurley, M. D.; Schneider, W. F.; Sehested, J.; Nielsen, O. J. *J. Phys. Chem.* **1993**, *97*, 7606.
(24) Wallington, T. J.; Hurley, M. D. *Chem. Phys. Lett.* **1992**, *189*, 437.
(25) Braun, W.; Herron, J. T.; Kahaner, D. K. *Int. J. Chem. Kinet.* **1988**, *20*, 51.
(26) Wallington, T. J.; Hurley, M. D.; Schneider, W. F.; Sehested, J.; Nielsen, O. J. *Chem. Phys. Lett.* **1994**, *218*, 34 and references therein.
(27) Tuazon, E. C.; Atkinson, R.; Corchnoy, S. B. *Int. J. Chem. Kinet.* **1992**, *24*, 639.
(28) Rowley, D. M.; Lesclaux, R.; Lightfoot, P. D.; Nozière, B.; Wallington, T. J.; Hurley, M. D. *J. Phys. Chem.* **1992**, *96*, 4889.
(29) Wallington, T. J.; Hurley, M. D.; Shi, J.; Maricq, M. M.; Sehested, J.; Nielsen, O. J.; Ellerman, T. *Int. J. Chem. Kinet.* **1993**, *25*, 651.
(30) Tschuikow-Roux, E.; Yano, T.; Niedzielski, J. *J. Chem. Phys.* **1985**, *82*, 65.
(31) Schneider, W. F.; Wallington, T. J. *J. Phys. Chem.* **1993**, *97*, 12783.
(32) Atkinson, R. *Atmos. Environ.* **1990**, *24A*, 1.
(33) Vaghjiani, G. L.; Ravishankara, A. R. *J. Phys. Chem.* **1989**, *93*, 1948.
(34) Cantrell, C. A.; Shetter, R. E.; Calvert, J. G.; Parrish, D. D.; Fehsenfeld, F. C.; Goldan, P. D.; Kuster, W.; Williams, E. J.; Westberg, H. H.; Allwine, G.; Martin, R. *J. Geophys. Res.* **1993**, *98*, 18355.